PHYSICAL ELECTRONICS

Original article
DOI: https://doi.org/10.18721/JPM.18408

THE EFFECT OF HEATING AND DRIFT OF ELECTRONS IN AN ELECTRIC FIELD ON THE ABSORPTION AND REFRACTION OF TERAHERTZ RADIATION IN ELECTRONIC INDIUM ANTIMONIDE

D. A. Karaulov, M. Ya. Vinnichenko✉*, V. A. Shalygin, D. A. Firsov*

Peter the Great St. Petersburg Polytechnic University, St. Petersburg, Russia

✉ mvin@spbstu.ru

Abstract. The calculation of the refractive index and absorption coefficient spectra has been performed for terahertz radiation (λ = 70 – 500 μm) in electronic indium antimonide (*n*-InSb) placed in an electric field of up to 200 V/cm. It was done on the basis of solving the Fresnel equation and the Boltzmann kinetic one. The Fermi – Dirac distribution shifted in velocity space was used as a nonequilibrium stationary electron distribution function over states. Changes in optical characteristics obtained in an electric field were shown to be due to the heating and drift of free electrons. The anisotropy of the electron distribution function over states in momentum space, arising in an electric field, leads to anisotropy of refraction and absorption; changes in the refractive index and absorption coefficient are different for radiation polarized parallel and perpendicular to the field. These changes differed for radiation polarized parallel and perpendicular to the field direction. This effect can be used for high-speed modulation of terahertz radiation because it is clearly pronounced.

Keywords: distribution function anisotropy, electron heating, electron drift, radiation absorption, radiation refraction, polarization of radiation, InSb

Funding: The reported study was funded by Russian Science Foundation (Grant No. 23-12-00036), https://rscf.ru/project/23-12-00036/.

Citation: Karaulov D. A., Vinnichenko M. Ya., Shalygin V. A., Firsov D. A., The effect of heating and drift of electrons in an electric field on the absorption and refraction of terahertz radiation in electronic indium antimonide, St. Petersburg State Polytechnical University Journal. Physics and Mathematics. 18 (4) (2025) 114–126. DOI: https://doi.org/10.18721/JPM.18408

Научная статья
УДК 535.34
DOI: https://doi.org/10.18721/JPM.18408

ВЛИЯНИЕ РАЗОГРЕВА И ДРЕЙФА ЭЛЕКТРОНОВ В ЭЛЕКТРИЧЕСКОМ ПОЛЕ НА ПОГЛОЩЕНИЕ И ПРЕЛОМЛЕНИЕ ТЕРАГЕРЦОВОГО ИЗЛУЧЕНИЯ В ЭЛЕКТРОННОМ АНТИМОНИДЕ ИНДИЯ

Д. А. Караулов, М. Я. Винниченко✉*, В. А. Шалыгин, Д. А. Фирсов*

Санкт-Петербургский политехнический университет Петра Великого, Санкт-Петербург, Россия

✉ mvin@spbstu.ru

Аннотация. На основе решения уравнения Френеля и кинетического уравнения Больцмана проведен расчет спектров показателя преломления и коэффициента поглощения терагерцового излучения (λ = 70 – 500 μm) в электронном антимониде индия (*n*-InSb) в электрическом поле напряженностью до 200 В/см. В качестве неравновесной стационарной функции распределения электронов по состояниям использовалось распределение Ферми –Дирака, смещенное в пространстве скоростей. Показано, что изменение оптических характеристик в электрическом поле связано с разогревом и дрейфом свободных электронов. Анизотропия функции распределения электронов по состояниям в импульсном пространстве, возникающая в электрическом поле, приводит к анизотропии преломления и поглощения; изменения показателя преломления и коэффициента поглощения различны для излучения, поляризованного параллельно направлению поля и перпендикулярно ему. Выраженность этого эффекта позволяет его использовать для малоинерционной модуляции излучения терагерцового диапазона спектра.

Ключевые слова: анизотропия функции распределения, разогрев электронов, дрейф электронов, поляризация излучения, InSb

Финансирование: Работа выполнена ***при финансовой поддержке*** Российского научного фонда (грант № 00036-12-23), https://rscf.ru/project/23-12-00036/.

Ссылка для цитирования: Караулов Д. А., Винниченко М. Я., Шалыгин В. А., Фирсов Д. А. Влияние разогрева и дрейфа электронов в электрическом поле на поглощение и преломление терагерцового излучения в электронном антимониде индия // Научно-технические ведомости СПбГПУ. Физико-математические науки. 2025. Т. 18. № 4. С. 114–126. DOI: https://doi.org/10.18721/JPM.18408

Introduction

An electric field can significantly affect the optical characteristics of semiconductors and semiconductor nanostructures. The majority of publications on electro-optical research consider the effect of an electric field on phenomena induced by bound electrons. Well-known phase electro-optical modulators are based on the Pockels effect in crystals without an inversion center, such as gallium arsenide (GaAs), cadmium telluride and zinc telluride (CdTe, ZnTe), as well as on the Kerr effect, which can also be observed in centrosymmetric materials, such as liquids and perovskites [1]. These effects lead to a change in the refractive index of the semiconductor associated with the crystal lattice. It is also possible to change the absorption coefficient and achieve amplitude modulation of radiation in an electric field by means of the Franz–Keldysh effect in bulk semiconductors [2] and the quantum-confined Stark effect in low-dimensional structures [3, 4].

Phenomena related to heating and drift of free charge carriers in an electric field are a separate group of electro-optical effects. Significantly lower electric fields are required for the system of free electrons to deviate from the equilibrium state compared to electrons bound to the ion core. An isotropic change in the electron distribution function over states in momentum space under an electric field (electron heating) leads to the modulation of the refractive index and absorption coefficient due to free electrons, which is independent of the radiation polarization.

The anisotropy of the distribution function associated with electron drift in an electric field leads to anisotropy of optical parameters; specifically, modulations of the refractive index and absorption coefficient differ for light polarized along and across the applied field. The effects of heating and drift of free electrons in an electric field are particularly substantial in semiconductors with high electron mobility, where the electronic indium antimonide (*n*-InSb) is the classical example.

The dependence of the refractive index in *n*-InSb on the electric field was experimentally determined in [5] for radiation with linear polarization parallel and perpendicular to the field. The experiments were carried out at the CO_2 laser wavelength (λ = 10.6 μm), where free electron absorption is negligible. The authors detected anisotropy of the refractive index induced by heating and electron drift. The obtained results were interpreted via a theoretical model approximating the nonequilibrium electron distribution function with the shifted Maxwell–Boltzmann distribution.

Optoelectronics and photonics of the terahertz range have been rapidly developing in recent years. Much attention is therefore focused on studying the anisotropy of the complex dielectric permittivity of indium antimonide in the terahertz range due to hot electron drift. Absorption of radiation by an ensemble of nonequilibrium electrons is significant in this range, so a new effect, which is the anisotropy of the absorption coefficient, can be expected to accompany the anisotropy of the refractive index induced by electron heating.

Indium antimonide was chosen as a model material because the band structure for this semiconductor is reliably established and the optical properties are studied in detail, making it possible to conduct accurate theoretical modeling to quantitatively compare its results with experimental data.

This paper reports on the theoretical calculation of the anisotropic refractive index and the anisotropic absorption coefficient for radiation in the terahertz range (wavelengths of 70–500 μm) in electronic indium antimonide in an electric field; the calculations were performed using the kinetic Boltzmann equation.

We obtained quantitative characteristics of the anisotropy of refractive index and absorption coefficient induced by an electric field. A nonequilibrium electron distribution function was used for the simulation in the shifted Fermi–Dirac distribution approximation, which is more correct for high doping levels than the Maxwell–Boltzmann distribution used in [5].

Calculation of refractive index and extinction coefficient

Consider the interaction of electromagnetic radiation characterized by the wave vector $\boldsymbol{\kappa}$ with an electronic indium antimonide (n-InSb) crystal under an applied electric field $\mathbf{E}$, in accordance with the schematic diagram in Fig. 1. Let us direct the electric field along a crystallographic direction with high symmetry, for example [111], and introduce a system of Cartesian coordinates.

To describe the optical properties of the sample, we introduce the dielectric permittivity tensor $\hat{\varepsilon}$, which includes the contribution of bound electrons and the lattice $\hat{\varepsilon}_L$, and the contribution of free electrons expressed in terms of the high-frequency conductivity tensor $\hat{\sigma}$:

$$\hat{\varepsilon}(\omega) = \hat{\varepsilon}_L + \frac{4\pi i}{\omega}\hat{\sigma}, \tag{1}$$

where ω is the frequency of electromagnetic radiation.

Note that the relatively low value of the electric field strength considered in this paper ($E \approx 100$–200 V/cm) does not affect the optical characteristics of InSb determined by bound electrons; the tensor $\hat{\varepsilon}_L$ can be treated as a scalar in the photon energy range $\hbar\omega < \varepsilon_g$ [6]:

$$\varepsilon_L = \varepsilon_\infty + \frac{\varepsilon_0 - \varepsilon_\infty}{1 - \left(\frac{\omega}{\omega_{\mathrm{TO}}}\right)^2 - i\frac{\omega\gamma_{\mathrm{TO}}}{\omega_{\mathrm{TO}}^2}}, \tag{2}$$

where ε_g is the band gap of InSb; ε_0, ε_∞ are the static and high-frequency values of the dielectric permittivity; ω_{TO} is the long-wavelength transverse optical (TO) phonon frequency; γ_{TO} is the damping constant related to the TO phonon lifetime τ_{TO} as $\gamma_{\mathrm{TO}} = 1/\tau_{\mathrm{TO}}$.

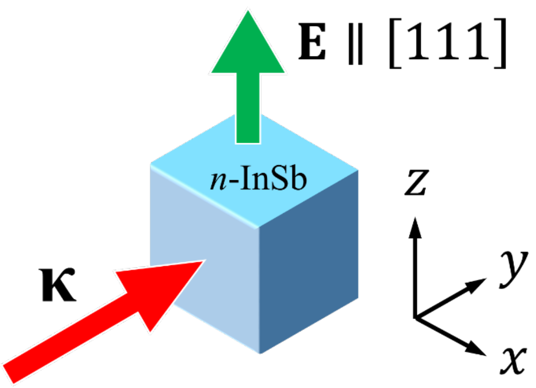

Fig. 1. Schematic diagram for propagation of radiation with wave vector $\boldsymbol{\kappa}$ in indium antimonide (n-InSb) sample placed in external electric field $\mathbf{E}$

The high-frequency conductivity tensor relates the electric field of a light wave E_ω and the free-electron current $\mathbf{J}_\omega$ induced by it:

$$J_{\omega i} = \sigma_{ij} E_{\omega j},\ i, j = x,y,z. \tag{3}$$

A constant external electric field **E** transforms indium antimonide into a uniaxial crystal with an optical axis directed along the field (in our case, along the z axis). Therefore, the $\hat{\sigma}$ tensor can be converted to diagonal form:

$$\hat{\sigma} = \begin{pmatrix} \sigma_{xx} & 0 & 0 \\ 0 & \sigma_{yy} & 0 \\ 0 & 0 & \sigma_{zz} \end{pmatrix}, \tag{4}$$

where $\sigma_{xx} = \sigma_{yy} \neq \sigma_{zz}$.

This holds true for the case of absence of an external magnetic field [7].

Transformation of Maxwell's equations, taking into account equalities (1)–(3), leads to the wave equation:

$$\nabla^2 \mathbf{E}_\omega = \frac{1}{c^2} \frac{\partial}{\partial t} \left(4\pi \hat{\sigma} \mathbf{E}_\omega + \varepsilon_L \frac{\partial \mathbf{E}_\omega}{\partial t} \right). \tag{5}$$

The solution to this equation is sought in the form of a plane wave:

$$\mathbf{E}_\omega(r, t) = (E_\omega \mathbf{e}_\omega) \exp[i(\boldsymbol{\kappa}\mathbf{r} - \omega t)], \tag{6}$$

where $\mathbf{e}_\omega$ is the unit polarization vector.

The wave vector $\boldsymbol{\kappa}$ is generally complex, and therefore it is convenient to introduce a complex refractive index $\tilde{n}$:

$$\boldsymbol{\kappa} = (\omega/c)\, \tilde{n}\mathbf{s}, \tag{7}$$

where **s** is a unit vector in the direction of wave propagation, while

$$\tilde{n} = n + ik_e. \tag{8}$$

The real part of the complex refractive index n is responsible for the wave phase velocity c/n, and the imaginary part k_e (extinction coefficient) appears in the expression for the absorption coefficient α:

$$\alpha = 2\omega \cdot k_e / c. \tag{9}$$

Substituting expression (6) into wave equation (5) leads to the following system of equations:

$$\sum_j \left(\tilde{n}^2 \delta_{ij} - \tilde{n}^2 s_i s_j - i \frac{4\pi}{\omega} \sigma_{ij} - \varepsilon_L \delta_{ij} \right) E_{\omega j},\ \ i, j = x, y, z. \tag{10}$$

This homogeneous system of equations has a nontrivial solution ($E_{\omega x}$, $E_{\omega y}$, $E_{\omega z}$) only if its determinant is equal to zero:

$$\det \left(\tilde{n}^2 \delta_{ij} - \tilde{n}^2 s_i s_j - i \frac{4\pi}{\omega} \sigma_{ij} - \varepsilon_L \delta_{ij} \right) = 0. \tag{11}$$

The equation (11) for $\tilde{n}^2$ is called the Fresnel equation. The Fresnel equation for the experimental configuration used (see Fig. 1) takes the form

$$\begin{vmatrix} \tilde{n}^2 - i\dfrac{4\pi}{\omega}\sigma_{xx} - \varepsilon_L & 0 & 0 \\ 0 & -i\dfrac{4\pi}{\omega}\sigma_{yy} - \varepsilon_L & 0 \\ 0 & 0 & \tilde{n}^2 - i\dfrac{4\pi}{\omega}\sigma_{zz} - \varepsilon_L \end{vmatrix} = 0. \quad (12)$$

Eq. (12) has two distinct solutions for $\tilde{n}^2$. Evidently, they correspond to the solutions of system (10) with two wave polarization directions: parallel and perpendicular to the applied electric field, which can be expressed in terms of the components of the dielectric permittivity tensor:

$$\mathbf{e}_\omega \parallel OZ \parallel \mathrm{E}:\ \tilde{n}_\parallel^2 = (n_\parallel + ik_{e\parallel})^2 = \varepsilon_L + \frac{4\pi i\sigma_{zz}}{\omega} = \varepsilon_{zz} \quad (13)$$

$$\mathbf{e}_\omega \perp OZ:\ \tilde{n}_\perp^2 = (n_\perp + ik_{e\perp})^2 = \varepsilon_L + \frac{4\pi i\sigma_{xx}}{\omega} = \varepsilon_{xx} \quad (14)$$

According to the terminology adopted for anisotropic media, a wave with polarization $\mathbf{e}_\omega \perp \mathbf{E}$ is ordinary, and a wave with polarization $\mathbf{e}_\omega \parallel \mathbf{E}$ is extraordinary.

Separating the real and imaginary parts in relations (13) and (14), we obtain systems of equations for the refractive index and the extinction coefficient for waves of the two polarization directions:

$$\begin{cases} n_\parallel^2 - k_{e\parallel}^2 = \mathrm{Re}\,\varepsilon_{zz}, \\ 2n_\parallel k_{e\parallel} = \mathrm{Im}\,\varepsilon_{zz}; \end{cases} \quad (15)$$

$$\begin{cases} n_\perp^2 - k_{e\perp}^2 = \mathrm{Re}\,\varepsilon_{xx}, \\ 2n_\perp k_{e\perp} = \mathrm{Im}\,\varepsilon_{xx}. \end{cases} \quad (16)$$

The solutions of these systems of equations have the following form:

$$\begin{cases} n_\parallel = \dfrac{1}{\sqrt{2}}\sqrt{\sqrt{(\mathrm{Im}\,\varepsilon_{zz})^2 + (\mathrm{Re}\,\varepsilon_{zz})^2} + \mathrm{Re}\,\varepsilon_{zz}}, \\ k_{e\parallel} = \dfrac{1}{\sqrt{2}}\sqrt{\sqrt{(\mathrm{Im}\,\varepsilon_{zz})^2 + (\mathrm{Re}\,\varepsilon_{zz})^2} - \mathrm{Re}\,\varepsilon_{zz}}; \end{cases} \quad (17)$$

$$\begin{cases} n_\perp = \dfrac{1}{\sqrt{2}}\sqrt{\sqrt{(\mathrm{Im}\,\varepsilon_{xx})^2 + (\mathrm{Re}\,\varepsilon_{xx})^2} + \mathrm{Re}\,\varepsilon_{xx}}, \\ k_{e\perp} = \dfrac{1}{\sqrt{2}}\sqrt{\sqrt{(\mathrm{Im}\,\varepsilon_{xx})^2 + (\mathrm{Re}\,\varepsilon_{xx})^2} - \mathrm{Re}\,\varepsilon_{xx}}. \end{cases} \quad (18)$$

If the condition $\sigma_{zz} \neq \sigma_{xx}$ is satisfied, then anisotropy of the optical parameters occurs: $n_\parallel \neq n_\perp$, $k_{e\parallel} \neq k_{e\perp}$.

Microscopic calculation of optical characteristics in an electric field

To establish how the electric field affects absorption and refraction of radiation in indium antimonide, we must find the components of the high-frequency conductivity tensor σ_{zz} and σ_{xx} (see Eqs. (13) and (14)). A common approach to determining the optical properties of a crystal associated with free electrons is to use the Drude model [8]. However, this model cannot easily account for the anisotropic electron distribution in momentum space under an electric field and the nonparabolicity of a conduction-band dispersion, both of which are essential for describing the heating and drift of free carriers induced by a constant electric field in this problem.

The components of the high-frequency conductivity tensor are determined using the solution of the kinetic Boltzmann equation for electrons in a constant electric field **E**, which induces heating and drift of electrons, and in a high-frequency electric field of an electromagnetic radiation wave $\mathbf{E}_\omega \exp(i\omega t)$. The equation for the electron distribution function $f(\mathbf{k}, t)$ has the following form in the approximation of relaxation time [9]:

$$\frac{\partial f}{\partial t} = -\frac{e}{\hbar}(\mathbf{E} + \mathbf{E}_\omega e^{i\omega t})\frac{\partial f}{\partial \mathbf{k}} + \frac{f - f_0}{\tau}, \tag{19}$$

where τ is the momentum relaxation time (for simplification, we assume it to be independent of the electron wave vector **k**), $f_0(\mathbf{k})$ is the equilibrium Fermi–Dirac distribution function.

The solution of Eq. (19) is sought as the sum of a stationary (nonequilibrium!) term and a high-frequency term:

$$f(\mathbf{k},t) = f_s(\mathbf{k}) + f_\omega(\mathbf{k})e^{i\omega t}. \tag{20}$$

If we assume that the electron–electron interaction is sufficiently strong, then the steady-state electron distribution function in a constant electric field can be represented as a Fermi–Dirac distribution $f_s(\mathbf{k})$ shifted in velocity space [10]. The parameters of this function are the electron temperature T_e, which is not equal to the lattice temperature T_0, and the drift velocity $\mathbf{v}_{dr}$:

$$\begin{cases} n_\perp = \dfrac{1}{\sqrt{2}}\sqrt{\sqrt{(\mathrm{Im}\,\varepsilon_{xx})^2 + (\mathrm{Re}\,\varepsilon_{xx})^2} + \mathrm{Re}\,\varepsilon_{xx}}, \\ k_{e\perp} = \dfrac{1}{\sqrt{2}}\sqrt{\sqrt{(\mathrm{Im}\,\varepsilon_{xx})^2 + (\mathrm{Re}\,\varepsilon_{xx})^2} - \mathrm{Re}\,\varepsilon_{xx}}. \end{cases} \tag{21}$$

Here $\varepsilon(\mathbf{k})$ is the law of electron energy dispersion, ε_F is the Fermi energy, and k_B is the Boltzmann constant.

We will use the isotropic Kane law of dispersion [11], which is a good approximation for indium antimonide:

$$\varepsilon(\mathbf{k}) = \frac{\varepsilon_g}{2}\left[\sqrt{1 + \frac{2\hbar^2 k^2}{m_e^0 \varepsilon_g}} - 1\right], \tag{22}$$

where m_e^0 is the effective electron mass at the bottom of the conduction band.

If we substitute expression (20) into Eq. (19), we can find the term $f_\omega(\mathbf{k})$ defining the transient part of the distribution function:

$$f_\omega(\mathbf{k}) = \frac{ie\mathbf{E}_\omega}{\hbar\left(\omega + \dfrac{i}{\tau}\right)}\frac{\partial f_s(\mathbf{k})}{\partial \mathbf{k}}. \tag{23}$$

The radiation-induced electric current of free electrons $\mathbf{J}_\omega$ is related to the high-frequency part of the distribution function as follows:

$$\mathbf{J}_\omega = -e\int \mathbf{v} f_\omega(\mathbf{k})\frac{2d\mathbf{k}}{(2\pi)^3} = e\int \frac{1}{\hbar}\frac{d\varepsilon}{d\mathbf{k}} f_\omega(\mathbf{k})\frac{2d\mathbf{k}}{(2\pi)^3}, \tag{24}$$

where the electron velocity is $\mathbf{v} = (1/\hbar)(d\varepsilon/d\mathbf{k})$.

Substituting expression (23) into Eq. (24), performing integration by parts, and comparing the result with equality (3), we find the components of the high-frequency conductivity tensor:

$$\sigma_{ii} = \frac{ie^2}{\left(\omega + \frac{i}{\tau}\right)} \int \frac{1}{\hbar^2} \frac{d^2\varepsilon}{dk_i^2} f_s(\mathbf{k}) \frac{2d\mathbf{k}}{(2\pi)^3}, \quad (25)$$

$$\sigma_{ij} = 0, \text{ if } i \neq j,\ i, j = x,y,z. \quad (26)$$

The expressions obtained for σ_{zz} and σ_{xx} can be used to calculate the behavior of the refractive index n, the extinction coefficient k, and the absorption coefficient α in an electric field for two directions of radiation polarization in accordance with expressions (13)–(18) and (9).

Simulation results and analysis

Refractive index anisotropy induced by the electric field and absorption coefficient anisotropy were simulated for n-type indium antimonide with the electron concentration $N_e = 5.4 \cdot 10^{15}$ cm^{-3} and a weak-field mobility $\mu = 1.5 \cdot 10^5$ cm^2/(V·s) (at a lattice temperature $T_0 = 78$ K). Experimental data are available on the electric field dependences of electron temperature and drift velocity for samples made of such a material, [5, 9], which facilitated the simulation.

The calculations used the known parameters of the band spectrum of InSb: $m^0_e = 0.014m_0$, ε_g(78 K) = 0.234 eV [12] and the dispersion of the dielectric permittivity of phonons: $\varepsilon_0 = 17.88$, $\varepsilon_\infty = 15.68$, $\hbar\omega_{TO} = 22.69$ meV, $\tau_{TO} = 4.1 \cdot 10^{-12}$ s [13].

The variations in the refractive index and absorption coefficient of indium antimonide induced by the electric field were calculated for the lattice temperature $T_0 = 78$ K. The following parameters of the nonequilibrium distribution function in an electric field are required to perform the calculations: electron temperature, drift velocity and position of the Fermi level of electrons included in expression (21) for the distribution function $f_s(\mathbf{k})$, as well as the strength of the applied electric field. Experimental results from [5] were used to find the electron temperature $T_e(E)$. We considered the variation in the refractive index of n-InSb depending on the applied electric field strength for the radiation wavelength of 10.6 μm. Comparing the experimental data with the calculation results, we obtained the dependence of electron gas heating $\Delta T_e = T_e - T_0$ on the electric field for the lattice temperature close to the boiling point of liquid nitrogen (77 K). The dependence $\Delta T_e(E)$ obtained by smoothing curves consisting of experimental points is shown in Fig. 2.

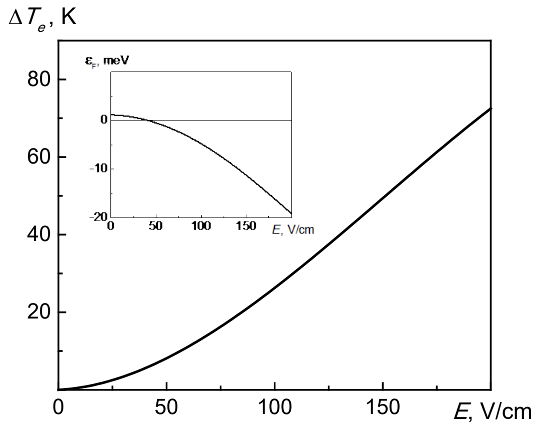

Fig. 2. Heating level of electron gas in n-InSb as a function of electric field strength. The lattice temperature is $T_0 = 78$ K, the electron concentration is $N_e = 5.4 \cdot 10^{15}$ cm^{-3}. *Inset*: field dependence of Fermi level position relative to the bottom of the conduction band

According to the results in [9], the field dependence of the drift velocity for the given material is close to linear in the region of electric fields less than 200 V/cm and can be calculated as $v_{dr} \approx \mu E$, where μ is the weak-field mobility.

The position of the Fermi level changes with the electric field. The value of ε_F for a given electric field was determined by normalizing the stationary distribution function $f_s(\mathbf{k})$ to the electron concentration N_e, which remains constant in the prebreakdown range of field strength values. The calculated dependence $\varepsilon_F(E)$ is shown in the inset to Fig. 2.

A convenient source of radiation for studying the effect of the electric field on the optical characteristics of materials in the terahertz range are continuous-wave gas lasers with optical pumping by radiation from another CO_2 laser, for example, a FIRL-100 laser from Edinburgh Instruments (UK) [14]. One of the most intense emission lines of this laser is the line with the wavelength $\lambda = 118.8$ μm. In view of this, we calculated the refractive index and absorption coefficient of indium antimonide in the electric field for radiation at this wavelength.

A constant electric field directed along the z axis determines the cylindrical symmetry of the problem. Therefore, it is convenient to carry out integration in Eq. (25) in the cylindrical coordinate system (k_ρ, k_z, φ). The transformation between Cartesian and cylindrical coordinates is as follows:

$$k_x = k_\rho \cos\varphi,\; k_y = k_\rho \sin\varphi,\; k_z = k_z. \tag{27}$$

Inverse relations:

$$k_\rho = \sqrt{k_y^2 + k_x^2}, \qquad \varphi = \mathrm{arctg}\left(\frac{k_y}{k_x}\right). \tag{28}$$

The law of dispersion (22) and the nonequilibrium distribution function (21) are written as follows in cylindrical coordinates:

$$\varepsilon(k_\rho, k_z) = \frac{\varepsilon_g}{2}\left[\sqrt{1 + \frac{2\hbar^2 (k_\rho^2 + k_z^2)}{m_e^0 \varepsilon_g}} - 1\right], \tag{29}$$

$$f_s(k_\rho, k_z) = \frac{1}{\exp\left[\dfrac{\varepsilon(k_\rho, k_z) - \hbar k_z v_{dr} - \varepsilon_F}{k_B T_e}\right] + 1}. \tag{30}$$

Consequently, the integrals defining the components of the high-frequency conductivity tensor (25) have the following form:

$$\begin{aligned}\int \frac{1}{\hbar^2}\frac{\partial^2 \varepsilon(k_\rho,k_z)}{\partial k_z^2} f_s(k_\rho,k_z)\frac{2d\mathbf{k}}{(2\pi)^3} &= \int \frac{1}{\hbar^2}\frac{\partial^2 \varepsilon(k_\rho,k_z)}{\partial k_z^2} f_s(k_\rho,k_z)\frac{2k_\rho dk_\rho d\varphi dk_z}{(2\pi)^3} = \\ &= 2\pi \int \frac{1}{\hbar^2}\frac{\partial^2 \varepsilon(k_\rho,k_z)}{\partial k_z^2} f_s(k_\rho,k_z)\frac{2k_\rho dk_\rho dk_z}{(2\pi)^3};\end{aligned} \tag{31}$$

$$\begin{aligned}&\int \frac{1}{\hbar^2}\frac{\partial^2 \varepsilon(k_\rho,k_z)}{\partial k_x^2} f_s(k_\rho,k_z)\frac{2d\mathbf{k}}{(2\pi)^3} = \\ &= \int \frac{1}{\hbar^2}\left(\frac{\partial^2 \varepsilon(k_\rho,k_z)}{\partial k_\rho^2}\cos^2\varphi + \frac{1}{k_\rho}\frac{\partial \varepsilon(k_\rho,k_z)}{\partial k_\rho}\sin^2\varphi\right) f_s(k_\rho,k_z)\frac{2k_\rho dk_\rho d\varphi dk_z}{(2\pi)^3} = \\ &= \pi \int \frac{1}{\hbar^2}\left(\frac{\partial^2 \varepsilon(k_\rho,k_z)}{\partial k_\rho^2} + \frac{1}{k_\rho}\frac{\partial \varepsilon(k_\rho,k_z)}{\partial k_\rho}\right) f_s(k_\rho,k_z)\frac{2k_\rho dk_\rho dk_z}{(2\pi)^3}.\end{aligned} \tag{32}$$

Integrals (31) and (32) were calculated numerically using the Newton–Cotes quadrature formulas.

The calculation results for ordinary ($\mathbf{e}_\omega \perp \mathbf{E}$) and extraordinary ($\mathbf{e}_\omega \parallel \mathbf{E}$) waves are shown in Figs. 3 and 4.

The physical nature of the influence of the electric field on the optical characteristics associated with free electrons can be qualitatively explained as follows. For a nonparabolic dispersion law, it is advisable to introduce an effective mass depending on the electron energy as follows:

$$\frac{1}{\hbar^2}\frac{\partial^2 \varepsilon}{\partial k_i^2} = \frac{1}{m_e(\varepsilon)},\quad i = x, y, z. \tag{33}$$

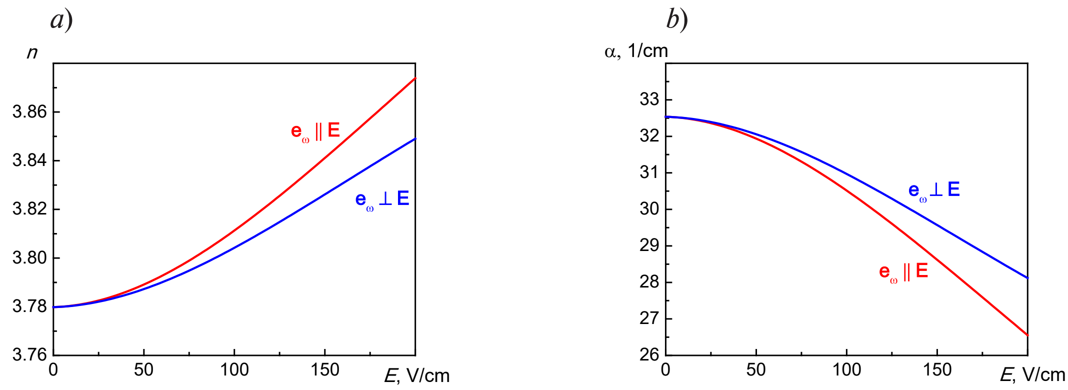

Fig. 3. Field dependences of refractive index (*a*) and absorption coefficient (*b*) for radiation of two mutually orthogonal linear polarizations. Emission wavelength λ = 118.8 μm

As the electron energy increases, this effective mass increases as well. Thus, the integral in expression (25) for the components of the tensor $\hat{\sigma}$ is the inverse effective mass averaged over the entire electron ensemble taking into account the nonequilibrium distribution function over states $f_s(\mathbf{k})$. Heating of electrons in the field increases the average electron energy, which leads to an increase in the average effective mass and to an isotropic decrease in the values of the components of the tensor $\hat{\sigma}$. As a result, refraction and absorption of radiation associated with free electrons are weakened. Since the contribution of free electrons to the refractive index is negative, the total refractive index increases with increasing field strength (see Fig. 3,*a*).

The anisotropy of the nonequilibrium distribution function $f_s(\mathbf{k})$ in momentum space, resulting from electron drift and heating, produces different values of the average inverse effective mass

$$\frac{1}{\hbar^2}\frac{\partial^2\varepsilon}{\partial k_z^2} \text{ and } \frac{1}{\hbar^2}\frac{\partial^2\varepsilon}{\partial k_x^2}.$$

This is reflected in the difference between the refractive index and the absorption coefficient for two orthogonal polarizations (see Fig. 3, *a* and *b*).

A better understanding of the effect of an electric field on the optical characteristics of the *n*-InSb crystal can be gained by analyzing the refractive index and absorption coefficient spectra, as well as the degree of their anisotropy in an electric field. The calculated spectral dependences are shown in Fig. 4.

Interestingly, a sharp peak induced by the electric field is observed on the refractive index anisotropy spectrum ($n_\parallel - n_\perp$) in the wavelength range of 250-270 μm. A negative peak is also observed in the spectral dependence of absorption coefficient anisotropy ($\alpha_\parallel - \alpha_\perp$). Evidently, these peaks are associated with the low-frequency plasmon–phonon resonance mode, which is typical for polar semiconductors [6]. In the absence of an external electric field, the plasma frequency ω_P is determined by the ratio

$$\omega_P^2 = \frac{4\pi e^2 N_e}{\varepsilon_\infty}\left\langle \frac{1}{m_e} \right\rangle, \tag{34}$$

where the angle brackets indicate the averaging of the inverse effective mass over the equilibrium Fermi–Dirac distribution function.

If $\omega_P << \omega_{TO}$ (which is true for the doping level under consideration), then the spectral position of the low-frequency plasmon–phonon mode ω_- can be calculated by the formula [15]:

$$\omega_- \approx \omega_P \frac{\varepsilon_\infty}{\varepsilon_0}. \tag{35}$$

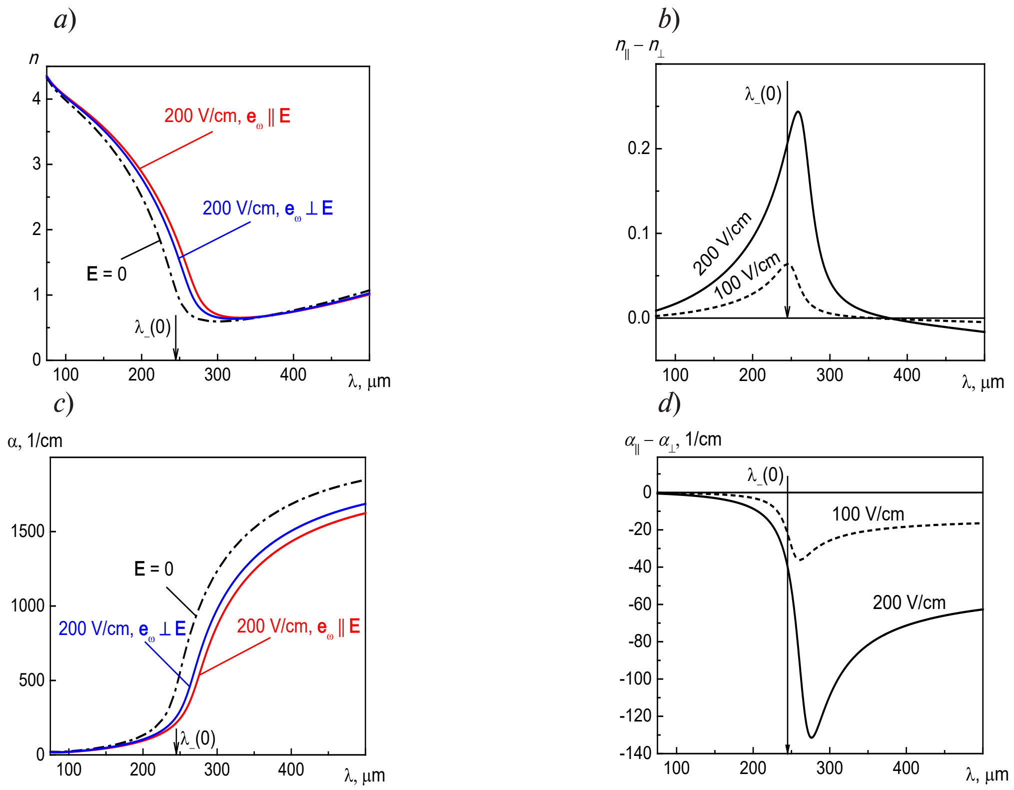

Fig. 4. Spectral dependences of optical parameters in equilibrium (E = 0 V/cm) and under applied electric fields: spectra of refractive index and its anisotropy, respectively (*a*, *b*); spectra of absorption coefficient and its anisotropy (*c*, *d*)
The vertical arrows in Fig. 4, *b*, *d* indicate the wavelength of the low-frequency plasmon–phonon mode at E = 0 V/cm

When an external electric field is applied, the magnitude of $\langle 1/m_e \rangle$ increases, and the frequencies ω_p and ω_- decrease, which is accompanied by long-wavelength shifts in the spectral curves of the refractive index and absorption coefficient. These shifts differ for radiation polarized parallel and perpendicular to the field (see Fig. 4, *a* and *c*). The spectral position of the low-frequency plasmon–phonon mode on the wavelength scale ($\lambda_- = 2\pi s/\omega_-$) in the absence of the electric field is marked in these figures as $\lambda_-(0)$. Note that peaks in the anisotropy spectra ($n_\parallel - n_\perp$) and ($\alpha_\parallel - \alpha_\perp$) are observed for the given field in the normal dispersion region, at wavelengths where the slope of the spectral curves $n_\parallel$ and $\alpha_\parallel$ reaches its maximum.

Analyzing the absorption coefficient spectra, we find that the quadratic dependence of absorption coefficient on radiation wavelength, characteristic for the Drude model, is observed at wavelengths below λ_-, but only in a narrow range (100–200 μm). This law is violated for shorter waves due to a noticeable contribution from the tail of the one-phonon resonance to absorption (see Eqs. (1) and (2)).

Fig. 3 shows the calculated field dependences of refractive index and absorption coefficient in *n*-InSb at 118.8 μm for two orthogonal polarizations. Analyzing Fig. 4, we can conclude that it is more expedient to conduct the experiment at wavelengths of 250–270 μm, where the effect is much more pronounced (in terms of the behavior of refractive index and absorption coefficient anisotropy).

Conclusion

We carried out model calculations of the refractive index and absorption coefficient for the terahertz range (λ = 70–500 μm) in electronic indium antimonide under an applied electric field. The optical characteristics exhibit different behavior in an electric field for radiation polarized parallel and perpendicular to the field. This results from the interplay of two factors: the nonparabolicity of the conduction band in indium antimonide and the anisotropy of the electron distribution function in momentum space, induced by electron heating and drift.

We demonstrated that an electric field not exceeding 200 V/cm induces a noticeable change in the optical characteristics, which should be used in developing high-speed electro-optical modulators of terahertz radiation.

REFERENCES

1. **Sinatkas G., Christopoulos T., Tsilipakos O., Kriezis E. E.,** Electro-optic modulation in integrated photonics, J. Appl. Phys. 130 (1) (2021) 010901.
2. **Oehme M., Schmid M., Kostecki K., et. al.,** The Franz – Keldysh effect in GeSn *p-i-n* diode, Appl. Phys. Lett. 104 (16) (2014) 161115.
3. **Bastard G., Brum J. A., Ferreira R.** Electronic states in semiconductor heterostructures (chapter), In book: H. Ehrenreich, D. Turnbull (Eds.) "Semiconductor heterostructures and nanostructures" (Book Ser. "Solid State Physics", Vol. 44), Academic Press, Cambridge (USA) (1991) 229–415.
4. **Podoskin A. A., Romanovich D.N., Shashkin I.S., et al.,** Switching control model of closed-mode structures in large rectangular cavities based on AlGaAs/InGaAs/GaAs laser heterostructures, Semiconduct. 54 (5) (2020) 581–586.
5. **Vorob'ev L.E., Stafeev V. I., Firsov D. A.,** Effect of heating and drift of electrons on refractive index of *n*-type InSb taking into account interband transitions, Fizika i Tekhnika Poluprovodnikov. 18 (3) (1984), 513–518 (in Russian).
6. **Chandrasekhar H. R., Ramdas A. K.,** Nonparabolicity of the conduction band and the coupled plasmon-phonon modes in *n*-GaAs, Phys. Rev. B. 21 (4) (1980) 1511–1525.
7. **Agranovich V. M., Ginsburg V. L.,** Crystal optics with spatial dispersion and excitons, Springer-Verlag, Berlin, 1984.
8. **Yu P. Y., Cardona M.,** Fundamentals of semiconductors. Physics and materials properties, 4-th edition, Springer-Verlag, Berlin, Heidelberg, 2010.
9. **Vorobev L. E., Komissarov V. S., Stafeev V. I.,** Faraday and Kerr effects of hot electrons in *n*-type InSb in the infrared (I), Phys. Status Solidi B. 52 (1) (1972) 25–37.
10. **Hammar C., Veissclas P.,** Hot electron polar scattering in InSb, Phys. Status Solidi B. 24 (2) (1967) 531–534.
11. **Anselm A. I.,** Introduction to semiconductor theory, Mir Publishing, Moscow, 2015.
12. **Littler C. L., Seiler D. G.,** Temperature dependence of the energy gap of InSb using nonlinear optical techniques, Appl. Phys. Lett. 46 (10) (1985) 986–988.
13. **Willardson R. K., Beer A. C.,** Semiconductors and semimetals. Optical properties of III–V compounds, Academic Press, New-York and London, 1967.
14. FIRL–Series–Datasheet: https://edin.becdn.net/wp-content/uploads /2024/ 07/FIRL-Series-Datasheet.pdf (Date of access is 14.10.2025).
15. **Orlov E. Yu., Melentev G. A., Shalygin V. A., Suihkonen S.,** Bulk plasmon-phonon polaritons in *n*-GaN, J. Phys. Conf. Ser. 816 (2017) 012004.

СПИСОК ЛИТЕРАТУРЫ

1. **Sinatkas G., Christopoulos T., Tsilipakos O., Kriezis E. E.** Electro-optic modulation in integrated photonics // Journal of Applied Physics. 2021. Vol. 130. No. 1. P. 010901.
2. **Oehme M., Schmid M., Kostecki K., et. al.** The Franz – Keldysh effect in GeSn *p-i-n* diode // Applied Physics Letters. 2014. Vol. 104. No. 16. P. 161115.
3. **Bastard G., Brum J. A., Ferreira R.** Electronic states in semiconductor heterostructures (chapter) // H. Ehrenreich, D. Turnbull (Eds.) "Semiconductor heterostructures and nanostructures" (Book Series "Solid State Physics", Vol. 44). Cambridge (USA): Academic Press, 1991. Pp. 229–415.
4. **Подоскин А. А., Романович Д. Н., Шашкин И. С., Гаврина П. С., Соколова З. Н., Слипченко С. О., Пихтин Н. А.** Модель управления конкуренцией замкнутых модовых структур в прямоугольных резонаторах большого размера на основе лазерных гетероструктур AlGaAs/InGaAs/GaAs // Физика и техника полупроводников. 2020. Т. 54. № 5. С. 484–489.

5. **Воробьев Л. Е., Стафеев В. И., Фирсов Д. А.** Влияние разогрева и дрейфа электронов на показатель преломления *n*-InSb с учетом межзонных переходов // Физика и техника полупроводников. 1984. Т. 18. № 3. С. 518–513.

6. **Chandrasekhar H. R., Ramdas A. K.** Nonparabolicity of the conduction band and the coupled plasmon-phonon modes in *n*-GaAs // Physical Review B. 1980. Vol. 21. No. 4. Pp. 1511–1525.

7. **Агранович В. М., Гинзбург В. Л.** Кристаллооптика с учетом пространственной дисперсии и теория экситонов. 2-е изд. М.: Наука, 1979. 432 с.

8. **Ю П., Кардона М.** Основы физики полупроводников. Пер. с англ. М.: Физматлит, 2002. 560 с.

9. **Vorobev L. E., Komissarov V. S., Stafeev V. I.** Faraday and Kerr effects of hot electrons in *n*-type InSb in the infrared (I) // Physica Status Solidi B. – Basic Solid State Physics. 1972. Vol. 52. No. 1. Pp. 25–37.

10. **Hammar C., Veissclas P.** Hot electron polar scattering in InSb // Physica Status Solidi B. – Basic Solid State Physics. 1967. Vol. 24. No. 2. Pp. 531–534.

11. **Ансельм А. И**. Введение в теорию полупроводников. СПб.: Лань, 480 .2025 с.

12. **Littler C. L., Seiler D. G.** Temperature dependence of the energy gap of InSb using nonlinear optical techniques // Applied Physics Letters. 1985. Vol. 46. No. 10. Pp. 986–988.

13. Оптические свойства полупроводников (Полупроводниковые соединения типа $A^{III} B^{V}$). Под ред. Р. Уиллардсона, А. Бира. Пер. с англ. М.: Мир, 1970. 488 с.

14. FIRL–Series–Datasheet: https://edin.becdn.net/wp-content/uploads /2024/ 07/FIRL -Series-Datasheet.pdf (Дата обращения: 14.10.2025).

15. **Orlov E. Yu., Melentev G. A., Shalygin V. A., Suihkonen S.** Bulk plasmon-phonon polaritons in *n*-GaN // Journal of Physics: Conference Series. 2017. Vol. 816. P. 012004.

THE AUTHORS

KARAULOV Danila A.
Peter the Great St. Petersburg Polytechnic University
29 Politechnicheskaya St., St. Petersburg, 195251, Russia
donil793@yandex.ru
ORCID: 0009-0002-1608-3659

VINNICHENKO Maxim Ya.
Peter the Great St. Petersburg Polytechnic University
29 Politechnicheskaya St., St. Petersburg, 195251, Russia
mvin@spbstu.ru
ORCID: 0000-0002-6118-0098

SHALYGIN Vadim A.
Peter the Great St. Petersburg Polytechnic University
29 Politechnicheskaya St., St. Petersburg, 195251, Russia
vadim_shalygin@mail.ru
ORCID: 0000-0001-6728-7286

FIRSOV Dmitry A.
Peter the Great St. Petersburg Polytechnic University
29 Politechnicheskaya St., St. Petersburg, 195251, Russia
firsov.da@spbstu.ru
ORCID: 0000-0003-3947-4994

СВЕДЕНИЯ ОБ АВТОРАХ

КАРАУЛОВ Данила Андреевич – *ассистент Высшей инженерно-физической школы Санкт-Петербургского политехнического университета Петра Великого.*
195251, Россия, г. Санкт-Петербург, Политехническая ул., 29
donil793@yandex.ru
ORCID: 0009-0002-1608-3659

ВИННИЧЕНКО Максим Яковлевич – *кандидат физико-математических наук, доцент Высшей инженерно-физической школы Санкт-Петербургского политехнического университета Петра Великого.*
195251, Россия, г. Санкт-Петербург, Политехническая ул., 29
mvin@spbstu.ru
ORCID: 0000-0002-6118-0098

ШАЛЫГИН Вадим Александрович – *доктор физико-математических наук, профессор Высшей инженерно-физической школы Санкт-Петербургского политехнического университета Петра Великого.*
195251, Россия, г. Санкт-Петербург, Политехническая ул., 29
vadim_shalygin@mail.ru
ORCID: 0000-0001-6728-7286

ФИРСОВ Дмитрий Анатольевич – *доктор физико-математических наук, профессор Высшей инженерно-физической школы Санкт-Петербургского политехнического университета Петра Великого.*
195251, Россия, г. Санкт-Петербург, Политехническая ул., 29
firsov.da@spbstu.ru
ORCID: 0000-0003-3947-4994

Received 15.10.2025. Approved after reviewing 27.10.2025. Accepted 27.10.2025.
Статья поступила в редакцию 15.10.2025. Одобрена после рецензирования 27.10.2025. Принята 27.10.2025.